i.e., the observed second-order rate constant $k_2 = k_a k_d/(k_{-a} + k_d)$.

The two limiting conditions (i) $k_d \gg k_{-a}$ and (ii) $k_d \ll k_{-a}$ are alternative ways of representing the situations where (i) the bond-making transition state lies highest and (ii) the bond-breaking transition state lies highest. In case i the expression reduces to $k_2 = k_a$ and the influence of chelation on bond breaking would be negligible, while in case ii it reduces to $k_2 = k_a k_d/k_{-a}$. The sensitivity of the rate constant to the pK_a of the entering amine resides mainly in k_{-a}, the rate constant for the dissociation of the amine from the five-coordinate intermediate, rather than in k_a. Thus the strength of binding of the amine to platinum parallels its proton basicity, and this must be reflected in its dissociative lability; i.e., k_{-a} decreases as the proton basicity of the amine increases. In this way k_2 will increase as the proton basicity of the amine increases. k_a may also be sensitive to amine basicity but rarely to the same extent, and there are even cases where k_2 actually decreases as the basicity of a heterocyclic amine increases.[17] The proton basicity is important in that part of the process where the amine moves from its fully bound to its partially bound state and far less important in the longer range interactions where it moves from an unbound state to a partially bonded state.[18]

The difference in the values of α for the reactions of the chelated ($\alpha = 0.58$) and monodentate ($\alpha = 0.41$) sulfoxides probably represents the greater assistance given to the more different bond-breaking step in the chelate complex by the amine when bound to the platinum (i.e., a dependence of k_d[19] upon the nature of the entered amine).

It follows that any discussion of nucleophilicity, which is effectively defined as a measure of k_2 rather than k_a, must take account of the relative importance of the bond-making and bond-breaking aspects of the substitution process. We propose to discuss this problem in a broader context elsewhere.

Acknowledgment. We thank Professor P. Uguagliati for some kinetic computing and the Italian Council of Research, CNR, Rome, for financial support in a bilateral project.

Registry No. *cis*-[Pt(Me_2SO)(py)Cl_2], 20647-45-4; *cis*-[Pt(Me_2SO)(2-Me-py)Cl_2], 61551-15-3; *cis*-[Pt(Me_2SO)(pyridazine)Cl_2], 76479-91-9; *cis*-[Pt(Me_2SO)(pyrimidine)Cl_2], 76479-92-0; *cis*-[Pt(Me_2SO)(4-CN-py)Cl_2], 76479-93-1; *cis*-[Pt($(Me_2SO)_2$)Cl_2], 22840-91-1; 4-Me-py, 108-89-4; py, 110-86-1; pyridazine, 289-80-5; 4-CN-py, 100-48-1; pyrimidine, 289-95-2; pyrazine, 290-37-9; 3,4-Me_2-py, 583-58-4; 3,5-Me_2-py, 591-22-0; 3-Me-py, 108-99-6; 2,4-Me_2-py, 108-47-4; 2-Me-py, 109-06-8.

Supplementary Material Available: A table of first-order rate constants (2 pages). Ordering information is given on any current masthead page.

---

(17) Gosling, R.; Kennedy, B. P.; Tobe, M. L. *Inorg. Chem.* **1977**, *16*, 1744.

(18) Romeo, R.; Tobe, M. L. *Inorg. Chem.* **1974**, *13*, 1991.

(19) We wish to thank one of the reviewers for helping us to focus our attention upon this point.

Contribution from the Department of Chemistry and Molecular Structure Center,
Indiana University, Bloomington, Indiana 47405

The Molybdenum–Molybdenum Triple Bond. 8.[1] Bis(6-methyl-2-pyridyl)methyltetrakis(dimethylamido)dimolybdenum

M. H. CHISHOLM,* K. FOLTING, J. C. HUFFMAN, and I. P. ROTHWELL

Received July 25, 1980

$Mo_2Cl_2(NMe_2)_4$ reacts in hydrocarbon solvents with a suspension of (6-methyl-2-pyridyl)methyllithium to give the title compound which has been obtained as a yellow crystalline solid by recrystallization from hexane solutions. In the solid state, each molybdenum atom is coordinated to two amido nitrogen atoms and the carbon atom of the (6-methyl-2-pyridyl)methyl anion, $-CH_2$pyMe. The halves of the molecule are joined by an unbridged Mo-to-Mo triple bond of distance 2.204 (1) Å and the central $Mo_2N_4C_2$ unit adopts the gauche ethane-like conformation with C_2 symmetry. The pyridine nitrogen is not coordinated to the Mo_2^{6+} center, a fact which is attributed to electronic rather than steric factors. ^{1}H NMR studies show the presence of two isomers in toluene-d_8. The spectra of the major isomer are consistent with the gauche conformation of the molecule found in the solid state; the spectra associated with the minor isomer are consistent with those expected for the anti rotamer. These observations are compared with those reported previously for bis(2-oxy-6-methylpyridine)tetrakis(dimethylamido)dimolybdenum. Crystal data for $Mo_2N_6C_{22}H_{40}$: space group $P2_1/a$; $Z = 4$; $a = 22.013$ (5), $b = 7.974$ (2), $c = 14.933$ (3) Å; $\beta = 96.43$ (1)°; $V = 2604.7$ Å^3; $d_{calcd} = 1.480$ g/cm^3.

Introduction

As a part of our continuing studies of the coordination chemistry surrounding the dinuclear metal centers $(M{\equiv}M)^{6+}$, where M = Mo and W,[2] we have embarked upon the synthesis and characterization of a series of compounds of general formula $M_2X_4(Y\text{-}L)_2$, where X = R (alkyl), NR_2, and OR and Y-L represents a uninegative and potentially bidentate ligand. We intend to investigate the Lewis acidity of these dimetal centers as a function of X and the donor ligand atom of potentially bidentate ligand Y-L. We report here the preparation of the compound where X = NMe_2 and Y-L is the uninegative ligand

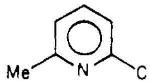

which is derived from deprotonation of 2,6-dimethylpyridine.

Results and Discussion

Synthesis. $Mo_2Cl_2(NMe_2)_4$ in hexane solution reacts slowly with a suspension of (6-methyl-2-pyridyl)methyllithium, $LiCH_2$pyMe, to give brown solutions and a finely divided precipitate of LiCl. Yellow crystals of the air- and moisture-sensitive title compound are obtained by crystallization of the hexane filtrate upon cooling. Analytical, infrared, and ^{1}H NMR data are reported in the Experimental Section.

Solid-State Structure. In the crystalline state, the compound is composed of discrete $Mo_2(NMe_2)_4(CH_2pyMe)_2$ molecules. Final atomic positional parameters are given in Table I, and bond distances and angles are given in Tables II and III ,

---

(1) Part 7: M. H. Chisholm, D. A. Haitko, J. C. Huffman, and K. Folting, *Inorg. Chem.*, **20**, 171 (1981).

(2) For recent reviews of the chemistry associated with these compounds, see M. H. Chisholm and F. A. Cotton, *Acc. Chem. Res.*, **11**, 356 (1978).

0020-1669/81/1320-1496$01.25/0

Table I. Fractional Coordinates for $Mo_2(NMe_2)_4(CH_2pyMe)_2$[a]

atom	10^4x	10^4y	10^4z	$10B_{iso}$, Å^2
Mo(1)	−401.7 (3)	2734 (1)	6812.2 (7)	11
Mo(2)	222.5 (3)	2502 (1)	8067.2 (4)	12
N(3)	9244 (3)	4950 (8)	6953 (4)	14
C(4)	−1219 (4)	5516 (11)	6244 (6)	18
C(5)	−606 (4)	6293 (10)	7619 (6)	18
N(6)	107 (3)	2230 (8)	5855 (4)	15
C(7)	−176 (3)	2481 (12)	4929 (5)	21
C(8)	764 (4)	1978 (12)	5850 (6)	21
N(9)	850 (3)	4177 (8)	7919 (4)	15
C(10)	1300 (4)	4512 (11)	8702 (6)	19
C(11)	924 (4)	5399 (11)	7205 (6)	21
N(12)	−327 (3)	2738 (8)	8997 (4)	16
C(13)	−961 (4)	3197 (11)	8997 (6)	20
C(14)	−38 (4)	2552 (12)	9938 (5)	23
C(15)	8961 (3)	676 (10)	6980 (6)	17
C(16)	−1629 (3)	1252 (9)	6507 (5)	15
N(17)	−1658 (3)	1467 (8)	5607 (4)	16
C(18)	−2169 (3)	2126 (10)	5151 (5)	20
C(19)	−2161 (4)	2357 (12)	4150 (6)	27
C(20)	−2669 (3)	2540 (10)	5589 (6)	21
C(21)	−2654 (3)	2308 (11)	6508 (6)	22
C(22)	−2131 (4)	1647 (10)	6976 (6)	20
C(23)	559 (4)	−46 (10)	7945 (6)	18
C(24)	1186 (4)	−26 (9)	8416 (5)	18
N(25)	1244 (3)	390 (8)	9317 (4)	17
C(26)	1808 (4)	563 (10)	9758 (6)	23
C(27)	1828 (4)	1102 (12)	10727 (6)	32
C(28)	2333 (5)	307 (13)	9356 (7)	34
C(29)	2284 (4)	−115 (12)	8449 (7)	32
C(30)	1707 (4)	−328 (11)	7974 (6)	23

[a] The isotropic thermal parameters listed for those atoms refined anisotropically are the isotropic equivalent. Numbers in parentheses in this and all following tables refer to the error in the least significant digits.

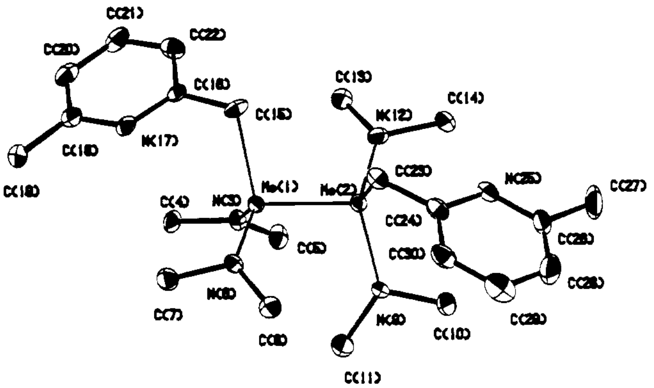

Figure 1. ORTEP view of the $Mo_2(NMe_2)_4(CH_2pyMe)_2$ molecule showing the atom numbering scheme used in tables. Atoms are represented by thermal ellipsoids drawn at the 50% probability level.

Figure 2. Stereoview of the $Mo_2(NMe_2)_4(CH_2pyMe)_2$ molecule viewed down the Mo–Mo axis. The virtual C_2 axis of symmetry is perpendicular to the Mo–Mo axis.

Table II. Bond Distances (Å) for the $Mo_2(NMe_2)_4(CH_2pyMe)_2$ Molecule

A	B	dist	A	B	dist
Mo(1)	Mo(2)	2.204 (1)	N(17)	C(18)	1.355 (10)
Mo(1)	N(3)	1.953 (6)	N(25)	C(24)	1.378 (10)
Mo(1)	N(6)	1.953 (6)	N(25)	C(26)	1.344 (10)
Mo(1)	C(15)	2.191 (8)	C(15)	C(16)	1.481 (10)
Mo(2)	N(9)	1.951 (6)	C(16)	C(22)	1.410 (11)
Mo(2)	N(12)	1.950 (6)	C(18)	C(19)	1.508 (11)
Mo(2)	C(23)	2.177 (8)	C(18)	C(20)	1.382 (11)
N(3)	C(4)	1.456 (9)	C(20)	C(21)	1.381 (12)
N(3)	C(5)	1.475 (10)	C(21)	C(22)	1.383 (11)
N(6)	C(7)	1.466 (9)	C(23)	C(24)	1.477 (11)
N(6)	C(8)	1.461 (10)	C(24)	C(30)	1.406 (11)
N(9)	C(10)	1.470 (10)	C(26)	C(27)	1.505 (12)
N(9)	C(11)	1.467 (10)	C(26)	C(28)	1.377 (13)
N(12)	C(13)	1.444 (10)	C(28)	C(29)	1.388 (14)
N(12)	C(14)	1.484 (10)	C(29)	C(30)	1.394 (13)
N(17)	C(16)	1.349 (10)			

Table III. Angles (Deg) for the $Mo_2(NMe_2)_4(CH_2pyMe)_2$ Molecule

A	B	C	angle
Mo(2)	Mo(1)	N(3)	101.7 (2)
Mo(2)	Mo(1)	N(6)	104.5 (2)
Mo(2)	Mo(1)	C(15)	100.7 (2)
N(3)	Mo(1)	N(6)	122.3 (3)
N(3)	Mo(1)	C(15)	113.4 (3)
N(6)	Mo(1)	C(15)	110.9 (3)
Mo(1)	Mo(2)	N(9)	103.2 (2)
Mo(1)	Mo(2)	N(12)	102.7 (2)
Mo(1)	Mo(2)	C(23)	101.1 (2)
N(9)	Mo(2)	N(12)	121.2 (3)
N(9)	Mo(2)	C(23)	112.2 (3)
N(12)	Mo(2)	C(23)	113.2 (3)
Mo(1)	N(3)	C(4)	117.3 (5)
Mo(1)	N(3)	C(5)	131.8 (5)
C(4)	N(3)	C(5)	110.6 (6)
Mo(1)	N(6)	C(7)	116.4 (5)
Mo(1)	N(6)	C(8)	133.0 (5)
C(7)	N(6)	C(8)	109.2 (6)
Mo(2)	N(9)	C(10)	117.2 (5)
Mo(2)	N(9)	C(11)	132.4 (5)
C(10)	N(9)	C(11)	109.8 (6)
Mo(2)	N(12)	C(13)	134.6 (5)
Mo(2)	N(12)	C(14)	115.5 (5)
C(13)	N(12)	C(14)	109.7 (6)
C(16)	N(17)	C(18)	119.6 (7)
C(24)	N(25)	C(26)	118.9 (7)
Mo(1)	C(15)	C(16)	104.6 (5)
N(17)	C(16)	C(15)	117.1 (7)
N(17)	C(16)	C(22)	121.0 (7)
C(15)	C(16)	C(22)	121.8 (7)
N(17)	C(18)	C(19)	116.4 (7)
N(17)	C(18)	C(20)	121.0 (7)
C(19)	C(18)	C(20)	122.6 (7)
C(18)	C(20)	C(21)	120.5 (7)
C(20)	C(21)	C(22)	118.6 (7)
C(16)	C(22)	C(21)	119.2 (8)
Mo(2)	C(23)	C(24)	105.0 (5)
N(25)	C(24)	C(23)	116.6 (7)
N(25)	C(24)	C(30)	120.5 (7)
C(23)	C(24)	C(30)	122.8 (8)
N(25)	C(26)	C(27)	115.2 (8)
N(25)	C(26)	C(28)	123.0 (8)
C(27)	C(26)	C(28)	121.7 (8)
C(26)	C(28)	C(29)	118.9 (9)
C(28)	C(29)	C(30)	119.6 (8)
C(24)	C(30)	C(29)	119.0 (8)

respectively. An ORTEP view of the molecule giving the atom numbering scheme is shown in Figure 1, and Figure 2 shows a stereoview of the molecule viewed down the Mo≡Mo bond.

The molecule adopts the gauche ethane-like conformation in the solid state and has a virtual, but not crystallographically imposed, C_2 axis of symmetry. There are two types of dimethylamido groups: those which are anti to C–Mo bonds and those which are mutually anti. The Mo–N bond distances are all very similar, however, and fall in the range 1.95–1.96

Å, typical of Mo–N distances in $Mo_2(NMe_2)_4X_2$ compounds. The Mo–C distances, 2.18 Å (averaged), are very similar to those found in $Mo_2Me_2(NMe_2)_4$[3] (2.175 (6) Å) and $W_2Me_2(NEt_2)_4$[4] (2.171 (11) Å), both of which have the anti conformation. Thus, there is no structural evidence of a trans influence[5] (perhaps more appropriately this should be called an anti influence) operating through the M–M bond. We do not expect to see such an effect, however, if the bonding in these ethane-like d^3–d^3 M≡M compounds is appropriately described by recent theoretical calculations,[6–9] since metal-metal bonds and metal–ligand bonds use different atomic orbitals of molybdenum. However, for dinuclear compounds having M–M triple bonds between two four-coordinate molybdenum atoms, a trans influence has been observed for metal–ligand bonds that lie in a plane at each end of the molecule. The origin of the trans influence in these molecules is readily understood in terms of the models advanced for square-planar mononuclear compounds,[5] since here again the metal–ligand and metal–metal orbitals use different metal atomic orbitals.

The Mo–Mo distance (2.204 (1) Å) is essentially the same as that in $Mo_2Me_2(NMe_2)_4$ which is 2.201 (1) Å[3] and shorter than that in $Mo_2(NMe_2)_6$ (2.214 (3) Å)[10] but longer than that found in $Mo_2(CH_2SiMe_3)_6$ (2.167 (?) Å).[11]

Within the context of the objective of this work, the single most interesting structural feature is the complete lack of coordination of the pyridine nitrogen atoms to the molybdenum atoms. The Mo–N(py) average distance is 3.25 Å. Furthermore, the Mo–C–C–N(py) torsional angles, which indicate the direction of the pyridine nitrogen atoms' lone pairs, are 60.4 and 64.9°. If the Mo–C–C–N(py) torsional angles were close to zero, then coordination to the $(Mo{\equiv}Mo)^{6+}$ unit along the Mo–Mo axis would be possible.

At this point, it is pertinent to question whether or not steric factors associated with the ligand prevent the pyridine nitrogen atoms from coordinating to the metal atoms. In order to investigate the role steric factors might play, we have considered two likely modes of pyridine nitrogen coordination. The first involves axial coordination (along the Mo–Mo axis); the second involves bridge formation. Simple models for each can be readily computer simulated.

1. Keeping the Mo–C–C and Mo–Mo–C angles fixed, a simple rotation about the CH_2–py bond to produce zero torsional angles for the Mo–C–C–N units generates a hypothetical molecule in which axial pyridine nitrogen coordination may be considered. With the bonding distances and Mo–C–C and Mo–Mo–C angles kept constant, the Mo–N(py) distances are 2.7 Å. Though this is too long to form a strong bond, relatively small changes of the Mo–Mo–C and Mo–C–C angles would allow this distance to come well within a bonding distance. For example, the $W_2(O_2CNMe_2)_6$ molecule has two weak and long W–O bonds (2.67 Å) aligned along the W–W axis.

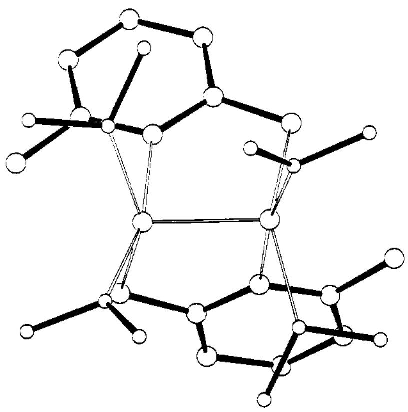

Figure 3. ORTEP drawing of the computer-simulated bridged $Mo_2(NMe_2)_4(CH_2pyMe)_2$ molecule viewed approximately along a C_2 axis of symmetry as found for the $Mo_2(NMe_2)_4(OpyMe)_2$ molecule.

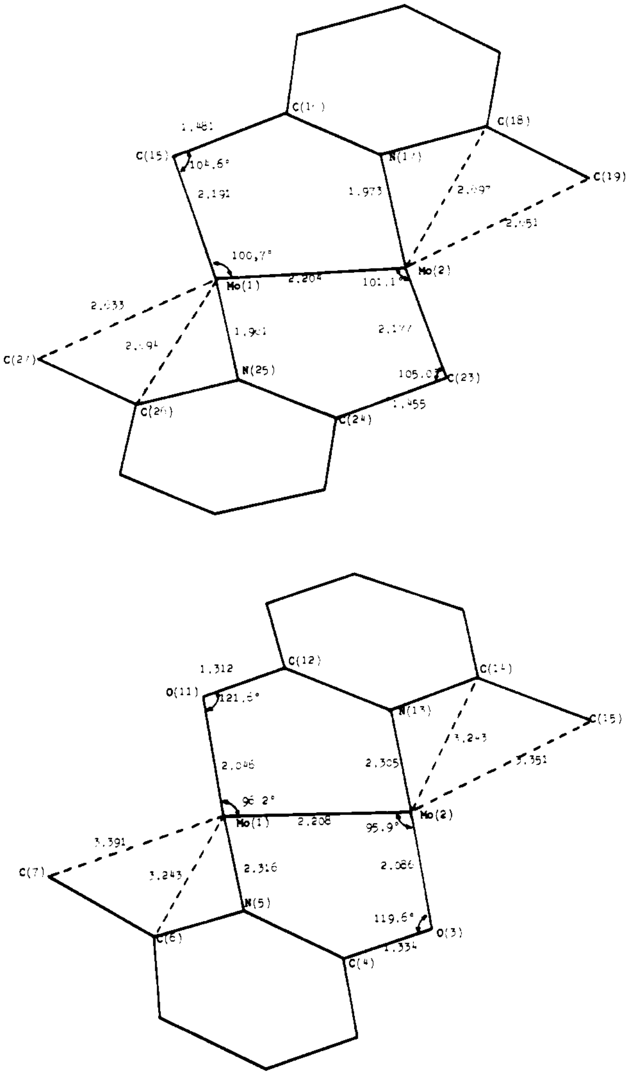

Figure 4. Comparison of the bridging skeleton found in $Mo_2(NMe_2)_4(OpyMe)_2$ and that of the computer-simulated $Mo_2(NMe_2)_4(CH_2pyMe)_2$ molecule.

2. A bridged form of the molecule can be simulated by keeping all bonding distances constant and rotating about the Mo–C bonds with zero torsional angles for the Mo–C–C–N(py) units. The chelating bridged structure has the two molybdenum atoms, and the carbon atoms and the nitrogen atoms associated with the bridging ligand contained within a plane. In order to accommodate a bis bridged structure, the Mo_2-

---

(3) M. H. Chisholm, F. A. Cotton, M. W. Extine, and C. A. Murillo, *Inorg. Chem.*, **17**, 2338 (1978).

(4) M. H. Chisholm, F. A. Cotton, M. W. Extine, M. Millar, and B. R. Stults, *Inorg. Chem.*, **15**, 2244 (1976).

(5) T. G. Appleton, H. C. Clark, and L. E. Manzer, *Coord. Chem. Rev.*, **10**, 337 (1973).

(6) F. A. Cotton, G. G. Stanley, B. J. Kalbacher, J. C. Green, E. Seddon, and M. H. Chisholm, *Proc. Natl. Acad. Sci. U.S.A.*, **74**, 3109 (1977).

(7) B. E. Bursten, F. A. Cotton, J. C. Green, E. A. Seddon, and G. G. Stanley, *J. Am. Chem. Soc.*, **102**, 4579 (1980).

(8) T. A. Albright and R. Hoffmann, *J. Am. Chem. Soc.*, **100**, 7736 (1978).

(9) M. B. Hall, *J. Am. Chem. Soc.*, **102**, 2104 (1980).

(10) M. H. Chisholm, F. A. Cotton, B. A. Frenz, W. W. Reichert, and L. W. Shive, *J. Am. Chem. Soc.*, **98**, 4469 (1976).

(11) F. Huq, W. Mowat, A. Shortland, A. C. Skapski, and G. Wilkinson, *Chem. Commun.*, 1079 (1971).

(12) M. H. Chisholm, F. A. Cotton, M. W. Extine, and B. R. Stults, *Inorg. Chem.*, **16**, 603 (1977).

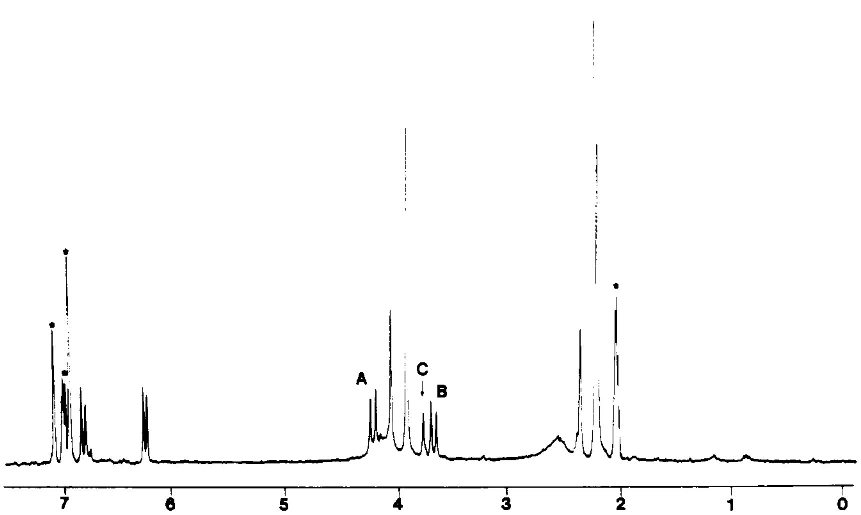

Figure 5. ^{1}H NMR spectrum of $Mo_2(NMe_2)_4(CH_2pyMe)_2$ recorded at 220 MHz, at -43 °C, and in toluene-d_8 showing the methylene protons of the CH_2pyMe ligands in the gauche rotamer, A and B, and the anti rotamer, C. At this temperature one pair of NMe_2 ligands of the gauche rotamer is not frozen out on the NMR time scale. The proton impurities in the toluene-d_8 are indicated by asterisks.

$(NC_2)_4$ skeleton of the molecule was assumed to be that observed in $Mo_2(NMe_2)_4$(2-oxy-6-methylpyridine)$_2$, which has two O–N bridges. Figure 3 shows a view of this hypothetical, computer-simulated molecule. At first glance, this seems a very plausible structure with an obvious parallel to that found for $Mo_2(NMe_2)_4$(2-oxy-6-methylpyridine)$_2$. However, certain differences are noteworthy. In Figure 4, a comparison of bond distances and interatomic nonbonding distances, together with pertinent bond angles, are shown. The computer-simulated bridged structure of $Mo_2(NMe_2)_4(CH_2pyMe)_2$ has much shorter Mo–N(py) bond distances, 1.973 and 1.961 Å. As a result, there are two ligand carbon atoms which come too close to each of the molybdenum atoms. The Mo–N distance and the nonbonding C-to-Mo distances are increased by merely enlarging the Mo–C–C angle from 105°.

Of course, none of these motions and structural changes would occur in isolation. Our purpose in generating these hypothetical structures is merely to emphasize that the (6-methyl-2-pyridyl)methyl ligand should be capable of forming bridged dimetal complexes, though, to our knowledge, none have been reported at this time.

While we discount the view that steric factors prevent py-N-to-Mo bond formation, we believe that there are two electronic factors which cause the $Mo_2(NMe_2)_4(2\text{-}YpyMe)_2$ molecules to have different structures.

First, though the anions formed by deprotonation of 2-hydroxy-6-methylpyridine and 2,6-dimethylpyridine may be described by the resonance forms **1a** and **1b**, the contribution

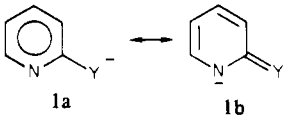

1a 1b

of **1b** is much smaller for Y = CH_2 than for Y = O. Accordingly, the basicity of the pyridine nitrogen is less for Y = CH_2 than for Y = O.

Second, the greater electronegativity of oxygen relative to carbon will increase the Lewis acidity of the metal atoms in $Mo_2(NMe_2)_4(OR)_2$ relative to $Mo_2(NMe_2)_4(CH_2R_2)$.

Both of these factors operate in the same direction and thus the $Mo_2(NMe_2)_4(CH_2pyMe)_2$ molecule behaves both in the solid state and in solution like the large class of $Mo_2R_2(NMe_2)_4$ compounds which have recently been characterized.[13]

^{1}H NMR Studies. The ^{1}H NMR spectrum of $Mo_2(NMe_2)_4(CH_2pyMe)_2$ in toluene-d_8 obtained at 220 MHz and -45 °C is shown in Figure 5. The spectrum is entirely consistent with the presence of a mixture of anti and gauche rotamers with the gauche being the predominant isomer. The methylene protons of the gauche rotamer are diastereotopic and give rise to an AB quartet, while, for the anti rotamer, they are equivalent because of the plane of symmetry which contains the C–Mo–Mo–C unit, and thus give rise to a single resonance in the ^{1}H NMR spectrum. There are three types of dimethylamide groups (two for the gauche and one for the anti isomer), and at -45 °C each type of NMe_2 group gives rise to two signals corresponding to proximal and distal methyl groups. When the temperature is raised, rotations about the Mo–N bonds become rapid, leading to the coalescence of proximal and distal methyl resonances, but anti $\rightleftharpoons$ gauche and gauche $\rightleftharpoons$ gauche (enantiomerization) is slow and not observed on the NMR time scale. These observations are analogous to those observed for other 1,2-dialkyldimolybdenum and -ditungsten (M≡M) compounds.[13]

Experimental Section

General procedures, including the preparation of $Mo_2Cl_2(NMe_2)_4$, have been described previously.[14] Note the use of dry and oxygen-free solvents and atmospheres.

Preparation of $Mo_2(NMe_2)_4(CH_2pyMe)_2$. To a suspension of $Mo_2Cl_2(NMe_2)_4$ (1.39 g, 3.17 mmol) in hexane (40 mL) was added (6-methyl-2-pyridyl)methyllithium (0.7 g, ≫2 equiv), and the resulting mixture was stirred at room temperature for 4 h. The brown mixture was filtered and the clear filtrate cooled to -15 °C in the refrigerator of the Dri-Lab apparatus. Yellow crystals of $Mo_2(NMe_2)_4(CH_2pyMe)_2$ (0.592 g, 33% yield on the basis of molybdenum) were collected by filtration and dried in vacuo. Anal. Calcd for $Mo_2N_6C_{22}H_{40}$: C, 45.52; H, 6.95; N, 14.48. Found: C, 45.71; H, 7.08; N, 14.62. IR data obtained from a Nujol mull between CsI plates in the region 2000–200 cm^{-1}: 1580 s, 1562 s, 1445 s, 1417 m, 1400 m, 1380 m, 1263 m, 1244 m, 1221 m, 1145 m, 1123 w, 1094 w, 1042 m, 1000 w, 985 w, 956 vs, 942 vs, 870 mw, 779 s, 739 m, 723 m, 645 m, 592 w, 555 m, 476 m, 406 w, 355 w, 339 m.

^{1}H NMR data obtained in toluene-d_8 at -43 °C and 220 MHz are as follows. (a) For the gauche rotamer: $\delta(NMe_2)$ = 3.96 and 2.26 with T_c = ca. 40 °C and 4.18 and 2.59 with T_c = -5 °C; for CH_2pyMe δ(Me) = 2.27, $\delta(CH_2)$ = 4.26 d and 3.72 d; δ(aromatic 3, 5) = 6.31 (d, J_{HH} = 7.0 Hz) and 6.86 (d, J_{HH} = 7.5 Hz); δ(aromatic 4) = 7.01 (t). (b) For the anti rotamer: $\delta(NMe_2)$ = 4.09 and 2.41 with $T_c \simeq$ 20 °C (the methyl and aromatic ligand proton resonances

---

[13] M. H. Chisholm and D. A. Haitko, *J. Am. Chem. Soc.*, **101**, 6784 (1979).

[14] M. Akiyama, M. H. Chisholm, F. A. Cotton, M. W. Extine, and C. A. Murillo, *Inorg. Chem.*, **16**, 2407 (1977).

are the same as those for the gauche rotamer; the methylene protons appear as a singlet at $\delta = 4.09$). δ values are in ppm relative to Me_4Si.

Preparation of (6-Methyl-2-pyridyl)methyllithium. To a hexane solution of *n*-butyllithium was added 2,6-dimethylpyridine by syringe. The solution was stirred, butane was evolved, and a yellow precipitate formed. This was collected by filtration, dried in vacuo, and stored in sealed ampules.

X-ray Structural Determination. A crystal of dimensions 0.05 × 0.24 × 0.30 mm was mounted in a nitrogen-filled glovebag and transferred to the liquid-nitrogen boil-off cooling system of the diffractometer.[15] The diffractometer utilized for data collection was designed and constructed locally. A Picker four-circle goniostat equipped with a Furnas Monochromator (HOG crystal) and Picker X-ray generator was interfaced to a TI 980 minicomputer, with Slo-syn stepping motors to drive the angles. Centering was accomplished with use of top/bottom–left/right slit assemblies. The minicomputer is interfaced by low-speed data lines to a CYBER 172-CDC 6600 multimainframe system where all computations are performed.

The cell dimensions obtained from 36 reflections at −171 °C with Mo Kα ($\lambda = 0.71069$ Å) were $a = 22.013$ (5) Å, $b = 7.974$ (2) Å, $c = 14.933$ (3) Å, $\beta = 96.43$ (1)°, $V = 2604.74$ Å^3, $Z = 4$, $d_{calcd} = 1.480$ g. cm^{-3}, and space group $P2_1/a$.

A total number of 6282 reflections were collected by using standard moving-crystal moving-detector techniques with the following values: scan speed = 5° min^{-1}, scan width = 1.6 + dispersion, single background time at extremes of scan = 4 s, aperture size = 3.0 × 4.0 mm. The limits of the data collection were $5° < 2\theta < 50°$. The number of reflections with $F > 2.33\sigma(F)$ was 3383 of the 4621 unique amplitudes. The data were corrected for absorption (linear absorption coefficient = 9.591 cm^{-1}); minimum and maximum corrections were 0.7980 and 0.9080, respectively.

The structure was solved by a combination of direct and Fourier methods to give final residuals $RF = 0.0709$ and $R_wF = 0.0560$. The goodness of the fit for the last cycle was 1.416, and the maximum δ/σ for the last cycle was 0.09.

All of the hydrogen atoms, except for those on the two methyl groups of the pyridine ligands [C(19), C(27)] were located and refined with use of isotropic thermal parameters. All nonhydrogen atoms were refined anisotropically.

The final difference map contained several peaks ranging from 0.6 to 0.9 e/Å^3 in the vicinity of C(19), and C(27), possibly indicative of a disorder or rotation of those methyl groups.

Acknowledgment. We thank the donors of the Petroleum Research Fund, administered by the American Chemical Society, the National Science Foundation, the Marshal H. Wrubel Computing Center, and the taxpayers of the State of Indiana for financial support of this work.

Registry No. $Mo_2(NMe_2)_4(CH_2pyMe)_2$, 76600-27-6; $Mo_2Cl_2(NMe_2)_4$, 63301-82-6; $LiCH_2pyMe$, 34667-18-0.

Supplementary Material Available: A table of anisotropic thermal parameters and a listing of observed and calculated structure factor amplitudes (32 pages). Ordering information is given on any current masthead page.

---

[15] J. C. Huffman, Ph.D Thesis, Indiana University, Bloomington, Ind., 1974.

Contribution from Donnan Laboratories, University of Liverpool, Liverpool L69 3BX, U.K.,
the Department of Chemistry, University of Glasgow, Glasgow G12 8QQ, U.K.,
the Department of Chemistry, University of Western Ontario, London, Canada N6A 5B7,
and the Inorganic Chemistry Laboratory, University of Oxford, Oxford OX1 3QR, U.K.

Synthesis, Structure, and Bonding in the Complex Cation $[Pt_2Me_3(\mu\text{-}Ph_2PCH_2PPh_2)_2]^+$: An Example of a Donor–Acceptor Metal–Metal Bond

MICHAEL P. BROWN,*[1a] SUSAN J. COOPER,[1a] AILEEN A. FREW,[1b] LJUBICA MANOJLOVIĆ-MUIR,*[1b]
KENNETH W. MUIR,[1b] RICHARD J. PUDDEPHATT,*[1c] KENNETH R. SEDDON,[1d] and MARY A. THOMSON[1c]

Received August 5, 1980

Several preparative routes to the binuclear trimethyldiplatinum complex cation $[Pt_2Me_3(\mu\text{-}Ph_2PCH_2PPh_2)_2]^+$, isolated as the PF_6^-, SbF_6^-, or ClO_4^- salts, have been found, and some aspects of the mechanism of formation from mononuclear precursors have been elucidated. The complex as the PF_6^- salt crystallizes in the space group $C_{2h}^5\text{-}P2_1/n$ with four molecules in a unit cell whose dimensions are $a = 10.220$ (4) Å, $b = 25.522$ (6) Å, $c = 23.832$ (3) Å, and $\beta = 93.57$ (3)°. On the basis of 5467 independent reflections with $I \geq 3\sigma(I)$, the structure was refined by full-matrix least-squares techniques to conventional agreement indices of $R = 0.081$ and $R_w = 0.13$. The complex cation contains a Pt–Pt separation of 2.769 Å formulated as a $Pt^{II} \rightarrow Pt^{II}$ donor–acceptor bond. This formulation is supported by consideration of the NMR coupling constants derived from analysis of the complex ^1H and ^{31}P NMR spectra. The Pt–Pt bond in this complex has a lower trans influence than Pt–Pt homopolar bonds in binuclear platinum(I) complexes.

Introduction

All known complexes of formula $[Pt_2X_2(Y)(dppm)_2]^{n+}$ (n = 0, 1; dppm = $Ph_2PCH_2PPh_2$), e.g., I–V, have "A-frame" structures, and the hydride $[Pt_2H_3(dppm)_2]^+$ (VI) is no exception even though the $Pt_2(\mu\text{-}H)$ grouping is electron deficient.[2,3] The existence of this trihydridodiplatinum complex cation prompted us to consider whether the trimethyldiplatinum complex cation $[Pt_2Me_3(dppm)_2]^+$ might exist and, if so, what type of structure it might have. On the one hand, it seemed unlikely that it would adopt an A-frame structure because that implied formation of an electron-deficient Pt_2-

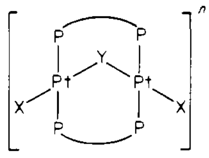

n = 0, X = Cl
I, Y = SO_2
II, Y = CH_2
III, Y = CO

n = 1, X = CH_3
IV, Y = Cl

n = 1, X = H
V, Y = SMe
VI, Y = H

---

[1] (a) University of Liverpool. (b) University of Glasgow. (c) University of Western Ontario. (d) University of Oxford.

[2] Brown, M. P.; Puddephatt, R. J.; Rashidi, M.; Seddon, K. R. *J. Chem. Soc., Dalton Trans.* **1978**, 516.

[3] (a) Brown, M. P.; Keith, A. N.; Manojlović-Muir, Lj.; Muir, K. W.; Puddephatt, R. J.; Seddon, K. R. *Inorg. Chim. Acta* **1979**, *34*, L223. (b) Brown, M. P.; Fisher, J. R.; Puddephatt, R. J.; Seddon, K. R. *Inorg. Chem.* **1979**, *18*, 2808.

0020-1669/81/1320-1500$01.25/0